Development of Copper Thermal Coefficient For Low Temperature Hybrid Bonding

Sefa Dag[1], Ming Liu[1], Liu Jiang[1], Amir Kiaee[1], Gilbert See[2], Prayudi Lianto[2], Buvna Ayyagari-Sangamalli[1], and El Mehdi Bazizi[1]

[1]*Design Technology, Applied Materials Inc., USA*
[2]*Applied Packaging Development Center, Applied Materials Inc., Singapore*
Sefa_dag@amat.com

***Abstract*— We present a modeling framework to guide the development and optimization of the hybrid bonding process. The key challenge is to achieve fully-bonded Cu-Cu metal interfaces/pads at low thermal budget such as 200-250 ºC to mitigate adverse thermal impact to the device structures. In this paper, we explore modification of the material coefficient of thermal expansion (CTE) and optimization with lower annealing temperature. To investigate new material solutions with a higher CTE, Classical Molecular Dynamics (CMD) simulation technique was implemented in the modelling framework. Two types of material modeling have been proposed for CTE improvement: *i)* Cu alloying; and *ii)* Cu capping. Simulation results show that copper alloying with selected metals can provide up to 40% improvement in CTE, and with capping, CTE can be improved up to 43% at optimal capping layer thickness. A continuum-scale thermo-mechanical model has been developed to study the Copper pad/pad interactions during the hybrid bonding process. Using this model, a parametric study is carried out on the effect of coefficient of thermal expansion (CTE) of different Copper alloys at low temperature regimes. The results show that CTE plays a significant role in bond quality and 40% improvement on CTE can facilitate the full Cu/Cu pad bonding at desired temperature regimes.**

Keywords — hybrid bonding, direct bonding, high-density interconnects, 3D integration, bump-less Cu-Cu, CTE, ab-initio, atomistic modeling, CMP, metal alloy, capping, dishing, continuum model, CMD, Thermo-mechanical.

I. INTRODUCTION

Heterogeneous integration chip technology is well known to increase system-level integration density while providing low power, highly reliable and flexible system design by integrating multiple chips and/or dies [1-4]. Hybrid bonding is one of the main advancements facilitating heterogeneous integration to achieve high-density interconnects. Figure 1 illustrates where hybrid-bonding is placed in packaging technology applications. Manufacturers currently employ thermal compression bonding (TCB) to stack and attach dies in packages, which has a limit of 10µm pitch. In contrast, electrical and mechanical analysis of hybrid-bonded interconnects shows it to be scalable down to 1µm pitch [5-7]. This bump-less approach is termed 'hybrid bonding' [8], since it involves bonding of not only the copper surfaces but also the surrounding dielectric. For optimal metal-to-metal connection, the bonding surface must be slightly recessed with respect to the surrounding dielectric surface and, as a result, requires stringent copper dishing tolerances on the chemical-mechanical polish (CMP) process integration [9]. This gap is designed to allow for Cu expansion during the post-bonding anneal step whereby the two Cu surfaces join to form a low interface-resistance electrical contact. A post-CMP copper dishing target depth of less than 5nm is required to achieve a bonding process yield of greater than 70% at an anneal temperature of 350ºC [10]. However, high anneal temperatures increase reliability concerns and can cause wafer or die damage [11]. In addition, the smaller interconnect pitch targets impose process challenges for accurate placement and stability of the bonded interconnect to achieve good bond yield and quality, as determined by electrical and thermo-mechanical reliability [12]. To form good metal-metal contacts at low temperature regimes, a higher coefficient of thermal expansion is required and, in addition, low-resistivity contacts require copper metallization. It is a non-trivial development effort to identify new metal treatments for copper that increase the thermal expansion rate without reducing the metal conductivity. The large parameter space and tight process targets required for a robust hybrid bonding process imposes a substantial experimental development resource. Therefore, this paper aims to present a modeling framework to optimize development of the metal thermal expansion rate by using ab-initio material simulation of various material designs, and using improved CTEs in thermo-mechanical reliability simulations[13]. The scale of analysis extends from the atomic effects to the system-level, ensuring comprehensive understanding and optimization of hybrid bonded interconnects.

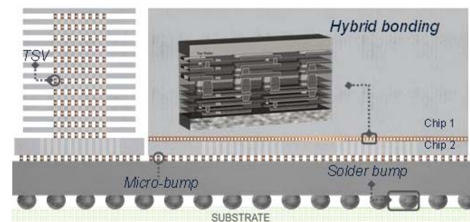

Fig. 1. System integration and PPAC benefits from optimal system level integration.

2377-5726/23/$31.00 ©2023 IEEE
DOI 10.1109/ECTC51909.2023.00064

This paper is divided into four sections. Section II describes the typical flow for hybrid bonding process, followed by a description of the modeling framework. Computational ab-initio based atomistic modeling is discussed in Section III and applied to the CTE development. Section IV presents the modeling of the thermo-mechanical reliability process to evaluate the bonding criteria.

II. Hybrid Bonding Process Flow and Modeling Framework

A. Hybrid Bonding Process Flow

Hybrid bonding can be realized as die-on-wafer or wafer-on-wafer. Each method has its benefits and drawbacks and vary slightly in the process flow[13]. The typical process flow for hybrid bonding is depicted in fig. 2. The incoming structure in fig. 2a shows the last die wiring metal layer with a deposited oxide and nitride etch stop layers. Fig. 2b shows the patterned metal pad. The pad and vias are metallized by physical vapor deposition (PVD) and electro-chemical deposition (ECD) steps. Accurately control of the plating thickness is not feasible, so copper is over-plated and planarized in a controlled manner using CMP. Finally, the die-to-wafer or wafer-to-wafer hybrid bonding is realized through dielectric bonding followed by annealing to bond the copper bumps.

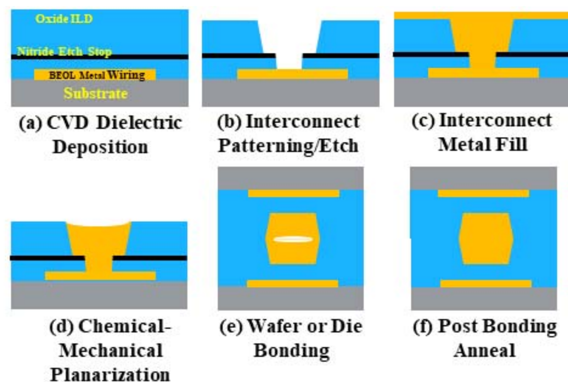

Fig. 2. Schematic of hybrid bonding process flow.

A holistic modeling framework is essential for the development of a new bonding technology such as hybrid bonding [13]. Without a systematic modeling framework, the development would consume too much time and resources to be feasible for the semiconductor industry's time-to-market demands. To address this need, a holistic modeling platform starting from material modeling and optimization, through systems modeling and optimization. This approach is referred to as Materials to Systems Co-Optimization (MSCO™). The MSCO™ platform focusses on materials, process, and interconnect co-optimization. The analyses in this paper cover part of the MSCO™ framework.

III. Atomistic Modeling

A. Computational Methods

Hybrid bonding is integral to 3D heterogeneous integration, but a lot of challenges remain in its development and evolution. An important aspect of overcoming the technological challenges is to understand, at the atomic level, the mechanisms determining material properties such as coefficient of thermal expansion and bonding processes. This work aims to elucidate the same to accelerate the development of hybrid bonding.

Coefficient of thermal expansion (CTE) is a material property that is indicative of the extent to which a material expands upon heating. Different materials with different substances expand by different amounts. In many experimental and theoretical studies carried out to date, CTE of the bulk material has generally been used [14-15]. Over small temperature ranges, thermal expansion of uniform linear objects is proportional to temperature change. Recent studies show CTE not only depends on metallic substances but also polycrystalline arrangement which may vary depending on the metal deposition conditions [16]. These polycrystalline metals are called as grained metals and each grain within the structure are joined at a grain boundary. Due to the complex nature of the applied treatments, it is difficult to correlate grain distribution with CTE of the structure [16]. This needs full research of experimental parameters to create an empirical environment using many trials. Such an approach would be complex, resource-intensive, and impractical given the short time-to-market requirements of a semiconductor process. This necessitates a simulation environment with well-defined computational techniques [17]. Our approach for better thermal characteristics is to create a Cu alloy with softer metal elements such as Al or Ag [18]. The mechanical and physical properties of materials are also determined by their chemical composition. It is well-known that metals containing dilute materials exhibit different solid strengthening or weakening arising from interactions between metals atoms and doping materials [19]. Some alloyed materials may be beneficial in terms of CTE improvement.

In this section, we used classical molecular dynamics (CMD) based simulation model to study the CTE with grain distribution and alloyed material dependency [16,17]. In addition, we investigated the effect of a copper surface cap layer with various elements to fulfill the requirements of hybrid bonding technology. Despite some pioneering insights, the design of new materials for hybrid bonding applications has remained heuristically based on trial and error. Only a limited number of candidate materials have been studied, given that manufacturing and testing of Cu alloys for hybrid bonding are time consuming and expensive. Providing guidance for the selection of high-performance alloys using theoretical and computational approaches is valuable and would greatly improve the search for new materials[13,16]. To date, there have been no comprehensive theoretical models that predict better CTE of certain Cu alloys as compared to pure copper. As a result, the initial goal is to identify the alloying elements that can be used for optimal CTE of the material under low-grain conditions and, alternatively, for the copper surface cap.

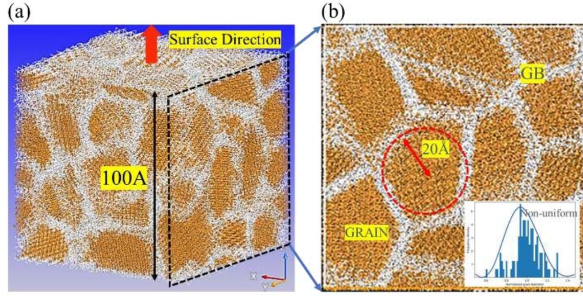

Fig. 3. (a) Atomistic model of Polycrystalline Copper. (b) Cross section shows grain distribution. We used 20 Å averaged grain size in simulation models. Grain size distribution is aligned with Poisson distribution.

Creating a simulation model for CMD simulations is the first step to successfully realize the polycrystalline bulk or surface. We initially implemented the polycrystalline structure by setting crystal size to 100Å×100Å×100Å to obtain a cubic supercell. The gap between grains was set to a small value, *e.g.* 0.1Å, to allow for a compact packing of the grains. Initial seed crystal is selected as Face Centered Cubic (FCC) Cu. A polycrystal generation tool was used to create grained structure. During the structural generation, uniform or non-uniform size distribution can be selected for various grain structure. Figure 3(a-b) shows randomly generated copper polycrystal model with 20 Å averaged grain distribution. Non-uniform grain distribution shows Poisson distribution which is shown in inset. Periodic boundary conditions are applied along x, y, and z directions for bulk model. For surface model, 100 Å vacuum space is added into simulation in z direction to mimic the slab behavior.

The next stage is to run the CMD for CTE extraction from the created model. For a CMD run, we used the suggested Embedded Atom Model (EAM) potential which is a suitable choice for Cu and alloying element[20]. In the first step of simulation, full geometry optimization is applied to remove potentially large interatomic forces resulting from the building procedure, before running the actual MD simulation. Force tolerance is set as 0.01 eV/Å. After full geometry optimization, long CMD run with NPT ensemble (constant pressure) for bulk copper and NVT ensemble for surface copper is applied at room temperature to get an equilibrated configuration for bulk and surface structures. At this stage, the reference structure is obtained with the reference thickness at room temperature. The obtained thickness at room temperature is also a reference thickness for CTE extraction. During the MD simulations, boundary conditions are applied to structures along x and y directions to keep the size of the structure constant, and z direction is set to relax with temperature dependence.

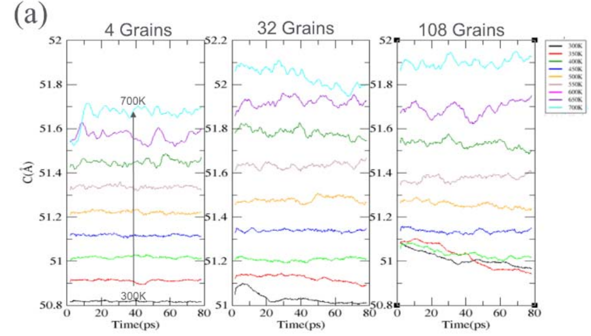

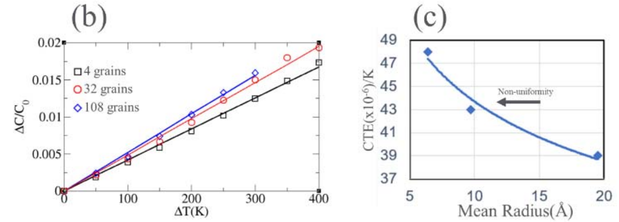

Fig. 4. (a) Temperature dependence of Copper thickness at various grain distributions. (b) Expansion rate with respect to temperature for various grain distributions. (c) Calculated CTE with respect to various grain distributions.

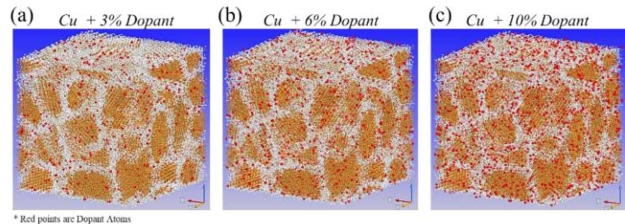

Fig. 5. (a) Atomistic model of Polycrystalline Copper. (b) Cross section shows grain distribution. We used 20 Å averaged grain size in simulation models. Grain size distribution is aligned with Poisson distribution.

After the equilibration process, system temperature is increased from 300 K to 700 K in 50 K increments and simulation time scale for each temperature step is 80 ps. Thickness of the configuration is measured at each MD time step and then average thickness is calculated. Figure 4(a) shows thickness change with respect to MD time steps for each grain distribution. Thickness oscillations at different temperature steps are shown in varying line colors. Average thickness, among 80 ps simulation time, increases with temperature for each grain distribution. Figure 4(a) clearly shows more expansion occurs with lower grain sizes. To see the temperature effect clearly, we also plotted expansion rate with respect to temperature changes for each grain distributions as shown in fig. 4(b). We found that expansion rate linearly increases with temperature change from 300 K to 700 K. Linearity is implied in this temperature range, since there is no clear phase change within the structure. The next step is to calculate the CTE of the materials from expansion rate change with respect to

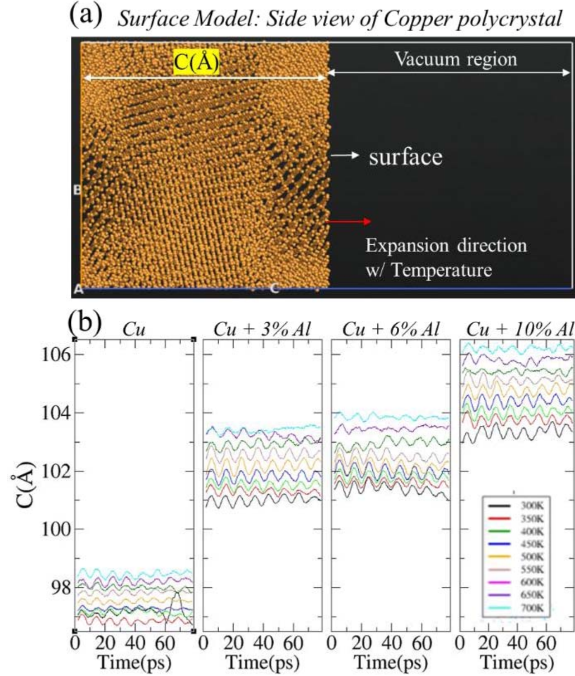

Fig. 6. (a) Atomistic model of surface presentation of copper polycrystal. (b) Surface thickness dependence with respect to simulation time at each temperature regime. Each section shows thickness change at different Al concentration.

Temperature which is shown in eq. 1. It is known that CTE of any given material is calculated with the expression:

$$CTE = \Delta(\frac{\Delta l}{l_o})/\Delta T$$

Eq. 1. This equation computes the CTE of a given material in one dimensional expansion.

Here, $\Delta l/l_o$, is thermal expansion rate and ΔT is temperature increase from 300 K. Figure 4(c) shows CTE change with respect to mean radius of grains. It is clearly shown that CTE of the bulk material increases with decreasing grain size. This implies that small, granulated metal deposition provides higher material CTE [16].

After establishing a reference Copper polycrystal model, we then focused on alloy models, including CuAl, CuAg, CuNi, CuSn and CuPb, then calculated CTE of these alloys for various concentrations from 3% to 10%. The conductivity of copper is an important reference for alloy selection since it is well-known that the conductivity of alloyed materials decreases if alloy materials concentration is too high. Furthermore, alloy concentration should be much lower than the solubility limit in copper. As a result, the intent is to calculate CTE of alloys at lower concentration regimes. Atomistic models of alloyed copper are shown in Figure 5. For each concentration, alloy materials are created with homogeneous atomic distribution in a copper superlattice.

Thickness measurement of surface copper at various conditions is a key to obtain mechanical characteristics. Figure 6(a) shows copper surface model which we removed the periodic boundary condition at the C axis and added enough vacuum space to mimic realistic surface characteristics and lowering imaginary interactions coming from long range electrostatic interactions. Figure 6(b) shows surface thickness change during MD simulations with respect to temperatures from 300 K to 700 K and various Al concentrations. A linear increase in thickness shows there are no structural transitions even under doping conditions. Figure 7(a) shows a linear increase of surface thickness with respect to Al concentration at room temperature. It is well-known that Cu atoms have weaker metallic bonds with Al atoms within the structure [21]. For this reason, averaged Cu-Al bonds (2.44 Å) are larger than Cu-Cu bonds (2.29 Å) [22]. Another effect on thickness expansion is Al-Al bonding which averages 2.6 Å. Both Cu-Al and Al-Al bonds have the most impact on lattice expansion. Figure 7(b) shows thickness expansion rate of pure copper and alloyed copper structures. $\Delta C/C_o$ linearly increases with temperature changes at every Al level.

B. Simulation Results and Discussion

The calculated CTE using Eq. 1 is shown in Fig. 8(a-d) for the various alloys and three different concentrations. As seen from the figure, four alloy materials, CuAl, CuAg, CuNi and CuSn, stand out as compared to baseline Cu. The CTE for all alloy conditions increases with the alloy concentration from 3% to 10%. The CTE for CuAl alloy saturate around 10% doping condition, and for CuAg alloy saturation occurs around 20%. On the other hand, CTE changes for CuNi and CuSn are still linear up to 10% regime. Another comparison is percentage of CTE change for each alloy with respect to pure Cu. The percentage increase in calculated CTE at 3% alloy conditions are 5.0%, 24%, 39.5% and 48% for CuNi, CuSn, CuAl and CuAg, respectively. These results show CuAg alloy is the best candicate material for high CTE improvement.

In hybrid bonding technology, another method to improve the bonding between metal pads is to use a cap layer on the copper surface. The bonding of copper surfaces is more difficult because copper tends to oxidize, especially at high temperatures. Cap layers rely on joining the copper pads with better cap-to-cap layer bonding. Therefore, CTE of the copper with cap material is the important physical quantity for hybrid bonding. In this section, we performed CTE extraction simulations for a copper surface capped with Silver (Ag) and Cobalt (Co) as a function of cap thickness from 10 Å to 40 Å. Figure 9(a-d) shows the model structures with capped copper. To maintain consistency between different models, total thickness of the structure is the same for each cap condition.

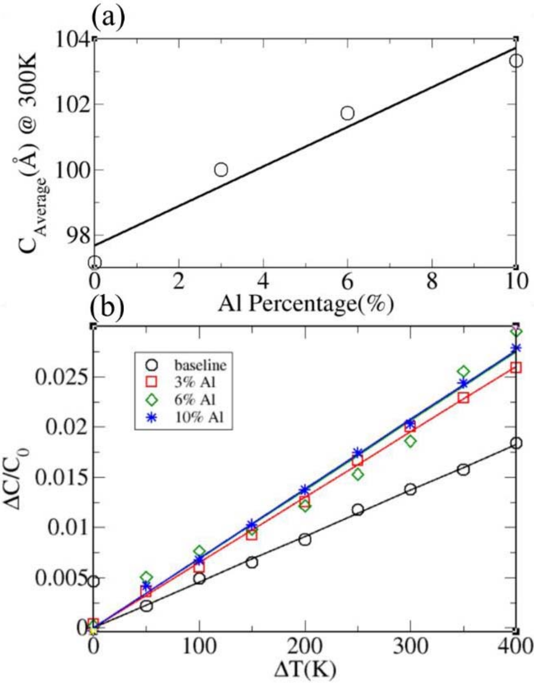

Fig. 7. (a) Change of averaqged thickness with respect to Al concentration at room temperature. (b) Copper linear expansion rate under various Al concentration.

Figure 10 (a-b) shows the extracted CTE changes with cap layer thickness. Calculated CTE is the combined CTE of Cu+cap layered structure. For both Ag and Co cap conditions, overall CTE is always larger than pure Cu CTE. This is due to a larger CTE of Ag and Co materials [18]. Another observation is the behavior of CTE changes with cap layer thickness. Both graphs show CTE of the full structure initially increases and then shows a decreasing trend with additional cap thickness increase. For Ag cap, joint CTE of the structure increases up to 41.5% when the proportional thickness between Ag and Cu is 0.2. For Co cap, we calculated similar characteristics. Joint CTE increases up to 43.6% when the proportional thickness between Co and Cu is 0.3. This is a characteristic behavior of thin-films. It is known that CTE of the thin films are always higher than its bulk value. When cap layer thickness increases beyond the thin-film thickness, the CTE of the cap layer will decrease and converge to its bulk value. As a result, in the case of a cap layer, there a characteristic layer thickness for optimal CTE increase.

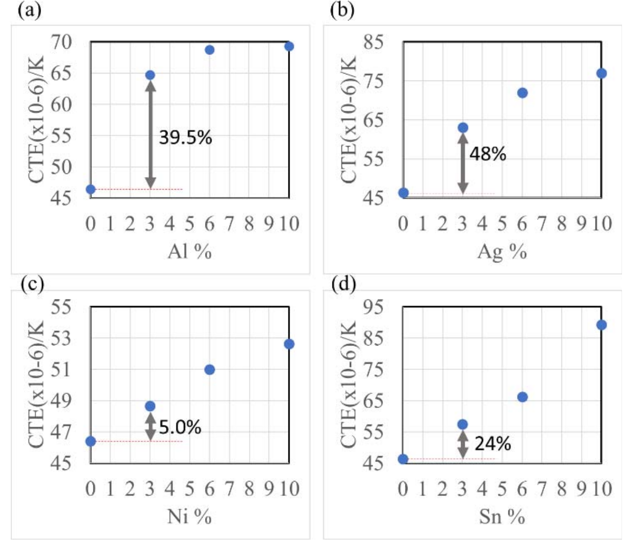

Fig. 8. Extracted CTE for (a) CuAl, (b) CuAg, (c) CuNi and (d) CuSn. Doping amounts are 3%, 6% and 10%.

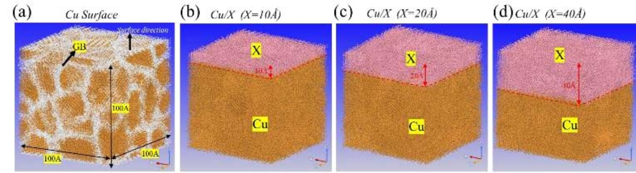

Fig. 9. Atomistic structure of capped copper. (a) pure copper surface (b) 10 Å capping thickness, (c) 20 Å capping thickness and (d) 40 Å capping thickness.

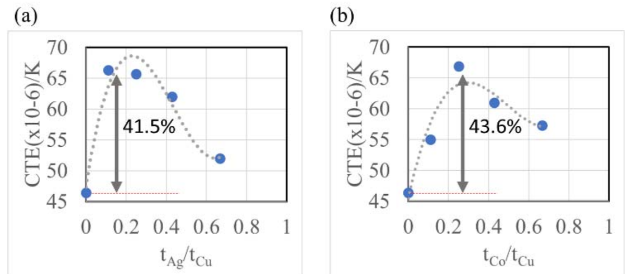

Fig. 10. Extracted CTE for (a)Cu-Ag bilayer and (b)Cu-Co bilayer models. CTE is plotted with respect to proportional thicknesses.

IV. Modeling for Thermomechanical Simulations

The key processing challenges for realizing hybrid bonding are achieving sub-nanometer surface roughness and precisely controlling copper dishing on the bonding surface. A well-controlled Chemical-Mechanical Polishing (CMP) process is required to enable shallow and uniform copper dishing. Dishing depth less than 5nm is required to achieve bonding yield of greater than 70% at bonding temperatures of 350ºC [23]. In this work, CMP processes at feature scale were simulated with models calibrated against experimental data. In addition, the dishing dependence on the Cu pad pattern was validated. Finally, simplification and optimization of the CMP process was carried out using this model.

It is well known that good Cu-Cu direct/hybrid bonding occurs at temperatures higher than 300˚C. A low thermal budget hybrid bonding process is desired to avoid damaging the wafer or die structures. However, it is challenging to achieve a fully bonded Cu-Cu interfaces at low thermal budget such as 200˚C-250˚C. We developed a continuum-scale thermo-mechanical model to study the Cu-Cu pad contact during the hybrid bonding process. Since CTE of the Cu pad is an important parameter, we conducted a parametric study to investigate the effect of CTE of different copper alloys at low anneal temperatures from 250°C to 300°C. Since grain size effects and alloying of copper with selected materials may provide up to 40% improvement in CTE, based on ab-initio simulations, we investigate the Cu-Cu hybrid bonding process with Cu CTE values within the range from bulk CTE (1x CTE) up to 1.4x CTE. To comprehensively understand the factors impacting the bonding quality for Cu-Cu interface, the pad size is also taken into consideration.

A. Model description

For the thermo-mechanical simulation, we prepared the Cu-Cu contact model. Equivalent dishing values for the top and bottom Cu pads is set to 10nm, which results in an initial gap between pads of 20nm. The diameters of top and bottom Cu pads are 3um and 5um respectively. The Cu-Cu contact structure is shown in the Fig.11. Due to symmetry of the structure, we simplified the Cu-Cu bonding structure to half to reduce computational expense. The structure was limited to the vertical displacement for top and bottom faces. The material properties [24,25] for all materials used in the simulation model are listed in the Table I.

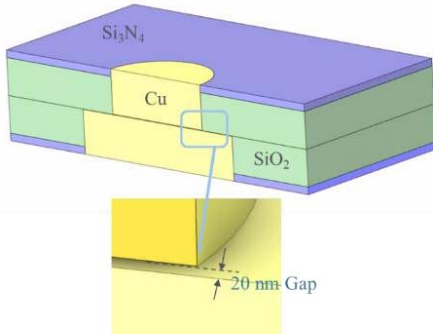

Fig. 11. Cu/Cu contact model surrounded with SiO2 and Si3N4 dielectrics. 10 nm dishing is used in initial condition.

TABLE I. MATERIAL PROPERTIES

Material	Cu	SiO_2	Si_3N_4
Young's Modulus (GPa)	110	75	150
Poison's Ratio	0.34	0.17	0.28
CTE (ppm/K)	18	0.5	2.6

We explored the impact of three parameters in the hybrid bonding process, including Cu CTE, annealing temperature and Cu pad diameter. To study the CTE impact on the hybrid bonding by considering the ab-initio simulation results, we gradually increased the Cu CTE from bulk value (1 CTE) up to 1.4 times the bulk value. A temperature profile shown in Fig. 12 is used in the model. The temperature is set to ramp up with 1˚C/min from 100˚C to 150˚C and dwell for 1 hour, then with the same rate, ramps up to the peak temperature (i.e., 250˚C, 300˚C and 350˚C) and dwells for 5 hours followed by a natural cooling process. To study the impact of pad size on bonding quality, we scaled down the structure to 50% and compared results with the original structure. We monitored the gap between Cu pads during the process.

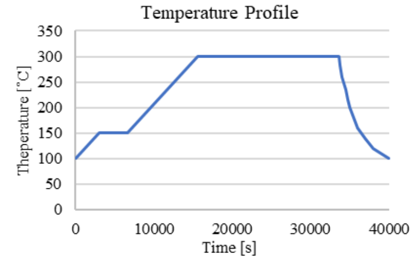

Fig. 12. Annealing temperature profile for thermo-mechanical simulation model.

A creep model was implemented for the Cu during the bonding process:

$$\dot{\varepsilon} = A^{*} e^{-(Q/RT)} \sigma^{n} t^{m^{*}} \quad (1)$$

where $\dot{\varepsilon}$ is the strain rate, A^{*} is a constant, Q is the activation energy in kJ·mol^{-1}, R is the universal gas constant, 8.314 J·mol^{-1}, T is temperature in K, σ is stress in MPa, n is stress exponent, t is time in s and m^{*} is time hardening exponent. Creep constants are listed in Table 2 [25, 26].

TABLE II. CREEP CONSTANTS

A^{*} [MPa^{-n}·s$^{-m^{*}-1}$]	1.43×10^{10}
n	2.5
m^{*}	-0.9
Q/R [K]	23695

B. Simulation Results

In this study, the gap between Cu pads at the end of the second dwell period was compared for different DOEs. We considered Cu-Cu bond occurs in the areas where the gap is equal or less than 0.1nm. For all figures in the study, the red color area is considered a Cu-Cu bond. Based on the simulation results, by increasing annealing temperature, the bonding/contact area increases accordingly. With 350˚C anneal temperature, the top and bottom copper pads came to a full contact. Lowering the annealing temperature to 300°C led to a

partial contact at the center of copper pads while the edges remained separated. It was observed that an anneal temperature of 250˚C was insufficient to close the gap for a full Cu-Cu bond. The TEM experimental data was used to validate the simulation results. Fig. 13 compares simulation results with TEM images for three annealing temperatures mentioned above. Based on the comparison, the simulation results align well with experimental data.

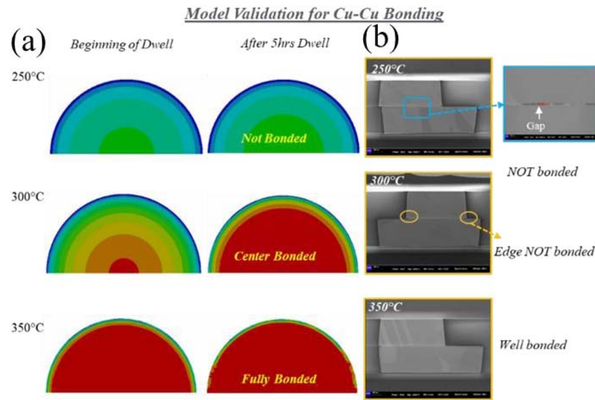

Fig. 13. (a) Bonding profile at Cu-Cu contact region at the beginning of dwelling and after 5 hours from dwelling from 250 ºC to 350 ºC. (b) TEM analysis shows various bonding scheme from different temperature regimes.

Since the Cu-Cu interface bonds well at 350˚C with bulk Cu CTE, we selected 300˚C as the baseline anneal temperature to test the CTE's impact on the bonding area by changing CTE values from bulk value to 1.4 times larger value. For the 300˚C annealing temperature, with bulk Cu CTE, the Cu pads formed a partial bond and the bonded area increases with increasing Cu CTE. The contact areas for each CTE value are shown in Fig. 14 (a), with a quarter of the structure presented. It shows that the bonded area propagates towards the Cu edge with higher CTE. Fig. 14 (b) shows the Cu-Cu bond for different Cu CTE values at the lower annealing temperature of 250˚C. Despite the Cu gap closure improvement by CTE increase, partial bonding occurred only at the highest CTE value. It suggests CTE increase could be a potential solution for Cu-Cu bonding quality improvement at lower thermal budget. Fig. 14 (c) shows the results of 50% smaller Cu pads at 300˚C anneal temperature. In this case, the gap between Cu pads is not filled despite the CTE increase. As the CTE value increases, the gap decreases from the center. In addition to CTE values, the model size would also proportionally impact the bonding areas.

The impact of annealing temperature can be observed by comparing Fig. 14 (a) and (b), where at 300 ˚C bonding occurs, however at 250˚C thermal expansion of Cu is insufficient to fill the gap and make a successful bonding. The results of current thermo-mechanical analysis proves that at the same annealing temperature, higher CTE values result in larger Cu-Cu bonding areas. Higher CTE values increase the chances of a fully bonded Cu-Cu interface at a lower thermal budget.

CTE (×factor)	(a) 300˚C	(b) 250˚C	(c) 300˚C (50% pad size)
1			
1.1			
1.2			
1.3			
1.4			

Fig. 14. Evolution of Cu-Cu bonding/gap with Cu CTE increase. Multiplication factor is used to show increament of CTE. Contact area improvement is also shown in temperatures from 250 ºC to 300 ºC.

As the CTE value of Cu alloys affects the Cu-Cu bonding, the size of the Cu pads may also impact the hybrid bonding quality. Another Cu-Cu interface model is generated based on 50% of the size of the baseline model.

V. Summary

A modeling framework for Cu/Cu bonding development has been presented. The framework comprehends ab-initio atomistic modeling for CTE extraction with various proposed material models and thermo-mechanical reliability model for Cu/Cu contact area calculation versus temperature. The computational ab-initio CMD simulations with EAM potentials have been used to extract the structural properties and temperature dependent structural changes of the given models. Our atomistic study also introduces a new recipe to perform CTE extraction simulations. Simulation results show Cu alloy with various metal elements are promising for Cu CTE improvement. CTE of Cu alloy with

Ag and Al improves by 48 and 39.5%, respectively. In addition, capping of the Cu surface with Ag and Co films also results in improved CTE of up to 43.6%. The cap film thickness plays a critical role for CTE improvement since CTE initially increases up to a critical thickness and then decreases. Finally, thermo-mechanical reliability in copper pads were analyzed for various temperature and CTE scenarios. Thermo-mechanical simulations clearly show that with the current dishing amount (10 nm), it is not possible to obtain good Cu-Cu bonding even at 300ºC with Cu CTE. Improved CTE from selective Cu alloy, improves the Cu-Cu bonding at 300°C. At lower annealing temperature of 250 ºC, the CTE increases similarly reduce the Cu-Cu gap and suggests a potential solution for success Cu-Cu bonding at lower thermal budget.

REFERENCES

[1] S. Naffziger *et al*., "Pioneering Chiplet Technology and Design for the AMD EPYC™ and Ryzen™ Processor Families: Industrial Product," *2021 ISCA*.

[2] F. Liang et al., "Development of Non-TSV-Interposer for High Electrical Performance Package," 2016 ECTC

[3] R. Mahajan et al., "Embedded Multi-die Interconnect Bridge -- A High Density, High Bandwidth Packaging Interconnect," 2016 ECTC.

[4] S. Ravichandran et al., "2.5D Glass-Panel-Embedded-Packages with Better I/O Density, Performance, Cost and Reliability than Current Silicon Interposers and High-Density Fan-Out Packages," 2018 ECTC

[5] A. Elsherbini, et al., "Hybrid Bonding Interconnect for Advanced Heterogeneously Integrated Processors," 2021 ECTC.

[6] A. Agrawal, et al., "Thermal and Electrical Performance of Direct Bond Interconnect Technology for 2.5D and 3D Integrated Circuits," 2017 ECTC.

[7] C. S. Tan and G. Y. Chong, "High throughput Cu-Cu bonding by non-thermo-compression method," in *Electronic Components and Technology Conference (ECTC), 2013 IEEE 63rd*, 2013, pp. 1158–1164

[8] V. Chidambaram, P. Lianto, X. Wang, G. See, N. Wiswell and M. Kawano, "Dielectric Materials Characterization for Hybrid Bonding," 2021 IEEE 71st Electronic Components and Technology Conference (ECTC), 2021, pp. 426-431, doi: 10.1109/ECTC32696.2021.00078.

[9] C. Sart et al., "Cu/SiO2 hybrid bonding: Finite element modeling and experimental characterization," 2016 6th Electronic System-Integration Technology Conference (ESTC), Grenoble, 2016, pp. 1-7, doi: 10.1109/ESTC.2016.7764484.

[10] C. Sart et al., "Cu/SiO2 hybrid bonding: Finite element modeling and experimental characterization", ESTC, 2016.

[11] M. Aoki, K. Hozawa, and K. Takeda, "Wafer-level hybrid bonding technology with copper/polymer co-planarization," in 3D Systems Integration Conference (3DIC), 2010 IEEE International, 2010, pp. 1–4.

[12] E. Beyne et al., "Scalable, sub 2μm pitch, Cu/SiCN to Cu/SiCN hybrid wafer-to-wafer bonding technology," 2017 IEEE International Electron Devices Meeting (IEDM), 2017, pp. 32.4.1-32.4.4, doi: 10.1109/IEDM.2017.8268486.

[13] Sitaraman, S. et al., "A Holistic Development Framework for Hybrid Bonding," 2022 IEEE 72nd Electronic Components and Technology Conference (ECTC), 2022, pp. 691-700, doi: 10.1109/ECTC51906.2022.00116.

[14] Ong, J-J. , et al,. "Low-Temperature Cu/SiO2 Hybrid Bonding with Low Contact Resistance Using (111)-Oriented Cu Surfaces", Materials, 2022, 15(5), 1888.

[15] Furuse, S., "Behavior of Bonding Strength on Wafer-to-Wafer Cu-Cu Hybrid Bonding", 2022 IEEE 72nd Electronic Components and Technology Conference (ECTC), San Diego, CA, USA, 2022, pp. 591-594, doi: 10.1109/ECTC51906.2022.00099.

[16] Dag, S., et al., "Material Innovation Through Atomistic Modelling for Hybrid Bonding Technology," 2022 IEEE 24th Electronics Packaging Technology Conference (EPTC), Singapore, Singapore, 2022, pp. 522-526, doi: 10.1109/EPTC56328.2022.10013200.

[17] S. Smidstrup et al., "QuantumATK: An integrated platform of electronic and atomic-scale modelling tools", J. Phys.: Condens. Matter 32, 015901 (2020).

[18] Engineering ToolBox, (2003). Thermal Expansion - Linear Expansion Coefficients. [online] Available at: https://www.engineeringtoolbox.com/linear-expansion-coefficients-d_95.html

[19] Bhaduri, A. (2018). Mechanical Properties and Working of Metals and Alloys. Germany: Springer Singapore.

[20] Daw, Murray S.; Foiles, Stephen M.; Baskes, Michael I. (1993). "The embedded-atom method: a review of theory and applications". Mat. Sci. Eng. Rep. 9 (7–8): 251. doi:10.1016/0920-2307(93)90001-U

[21] Wei, H.; Zhang, P.; Tang, Y. Ab Initio Molecular Dynamics Study of the Structure and Properties of Nb-Doped Zr-Cu-Al Amorphous Alloys. Metals 2021, 11, 1821. https://doi.org/10.3390/met11111821.

[22] Prasenjit Bag, Amelie Porzelt, Philipp J. Altmann, and Shigeyoshi Inoue, Journal of the American Chemical Society 2017 139 (41), 14384-14387, DOI: 10.1021/jacs.7b08890.

[23] C. Sart et al., "Cu/SiO2 hybrid bonding: Finite element modeling and experimental characterization," 2016 6th Electronic System-Integration Technology Conference (ESTC), 2016, pp. 1-7, doi: 10.1109/ESTC.2016.7764484.

[24] Y. Beilliard, R. Estevez, G. Parry, P. McGarry, L. D. Cioccio, and P. Coudrain, "Thermomechanical finite element modeling of Cu–SiO2 direct hybrid bonding with a dishing effect on Cu surfaces," *International Journal of Solids and Structures*, vol. 117, pp. 208–220, 2017, doi: https://doi.org/10.1016/j.ijsolstr.2016.02.041.

[25] Li, G., Thomas, B.G. & Stubbins, J.F. Modeling creep and fatigue of copper alloys. Metall Mater Trans A 31, 2491–2502 (2000). https://doi.org/10.1007/s11661-000-0194-z

[26] L. Ji, F. X. Che, H. M. Ji, H. Y. Li and M. Kawano, "Wafer-to-Wafer Hybrid Bonding Development by Advanced Finite Element Modeling for 3-D IC Packages," in IEEE Transactions on Components, Packaging and Manufacturing Technology, vol. 10, no. 12, pp. 2106-2117, Dec. 2020, doi: 10.1109/TCPMT.2020.3035652.